Can aerosols be trapped in open flows?

Rafael D. Vilela[1, *] and Adilson E. Motter[2]

[1]*Max Planck Institute for the Physics of Complex Systems, 01187 Dresden, Germany*
[2]*Department of Physics and Astronomy, Northwestern University, Evanston, IL 60208, USA*

The fate of aerosols in open flows is relevant in a variety of physical contexts. It is currently assumed that such finite-size particles always escape in open chaotic advection. Here we show that this is not the case. We analyze the dynamics of aerosols both in the absence and presence of gravitational effects, and both when the dynamics of the fluid particles is hyperbolic and nonhyperbolic. Permanent trapping of aerosols much heavier than the advecting fluid is shown to occur in all these circumstances. This phenomenon is determined by the occurrence of multiple vortices in the flow and is expected to happen frequently for realistic particle-fluid density ratios.

PACS numbers: 05.45.-a, 47.52.+j, 47.55.Kf

The question of whether finite-size particles escape or are trapped in open flows is relevant for microfluidics [1] and environmental processes [2]. In the former, the trapping enables the separation of particles according to their size, with applications in biology and medicine [3]. In the latter, the trapping of finite-size particles has consequences for the transport of pollutants and cloud droplets in the atmosphere [4, 5] and plankton in the ocean [5, 6].

In open flows displaying chaotic advection [7], fluid particles are injected into some domain containing a chaotic saddle [8], where they move chaotically for a finite amount of time until they finally escape. This is the history of *almost all the injected particles* in the very common and important case where the fluid is incompressible. The advection dynamics of point-like particles is then conservative [9]. When instead finite-size particles are injected into the domain, the outcome can be fundamentally different [10]. The reason is that these particles are subjected to new forces, in particular the Stokes drag. Their dynamics is dissipative, allowing the existence of attractors where the particles can be trapped. This has been shown to be typical in the case of *bubbles*, i.e., finite-size particles less dense than the fluid [11]. On the other hand, current results support the assumption that finite-size particles denser than the fluid, called *aerosols*, always escape [11, 12]. Moreover, there is evidence that aerosols escape even faster than the particles of fluid [11]. The physical reason for this distinct observed behavior is that the chaotic saddle is usually associated with the occurrence of vortices. Bubbles in vortices tend to move inwards, therefore possibly being trapped, whereas aerosols tend to move outwards, therefore escaping and possibly doing so faster than the fluid itself.

In this Letter, we show that the premise that aerosols in vortices tend to move outwards does not necessarily imply that these particles will always escape faster in open flows. More remarkably, we show that aerosols much heavier than the advecting fluid can be *permanently trapped* in open chaotic advection. The mechanism affording the trapping of aerosols is associated with the occurrence of two or more vortices in the flow. In escaping from a vortex, the aerosols may come to the domain of another vortex, which in its turn may drive the particles back to the first vortex. This may lead to the formation of bounded stable orbits that give rise to an attractor.

We start with the equation of motion for a small heavy spherical particle in a fluid flow. In dimensionless form, it reads [13]

$$\ddot{\mathbf{r}} = A\left(\mathbf{u} - \dot{\mathbf{r}} - W\mathbf{n}\right), \tag{1}$$

where $\mathbf{r}$ is the position vector of the particle, $\mathbf{u} = \mathbf{u}(\mathbf{r}(t), t)$ is the fluid velocity field evaluated at the particle's position, and $\mathbf{n}$ is a unit vector pointing upwards in the vertical direction. The two parameters governing the dynamics are the inertia parameter A and the gravitational parameter W. They can be written in terms of the characteristic length L and velocity U of the flow, radius a of the particle, kinematic viscosity ν of the fluid, gravitational acceleration g, and densities ρ_p and ρ_f of particle and fluid, respectively. The defining equations for these parameters are $W = (2a^2\rho_p g)/(9\nu U \rho_f)$ and $A = R/St$, where $R = \rho_f/\rho_p \ll 1$ and $St = (2a^2U)/(9\nu L)$ is the Stokes number of the particle. In the case of a droplet of water in the air, for example, we have $\rho_f/\rho_p \sim 10^{-3}$.

In order to demonstrate the occurrence of trapping of aerosols, we use the blinking vortex-source system [14], a prototypical flow model displaying open chaotic advection. This 2-dimensional system is periodic in time and consists of two alternately open point sources in a plane. It models the alternate injection of rotating fluid in a large shallow basin. The flow is described by the streamfunction

$$\Psi = -\left(K\ln r' + Q\phi'\right)\Theta(\tau) - \left(K\ln r'' + Q\phi''\right)\Theta(-\tau), \tag{2}$$

where $\tau = 0.5T - (t \bmod T)$. Here, r' and ϕ' are polar coordinates centered at $(x, y) = (-1, 0)$, while r'' and ϕ'' are polar coordinates centered at $(1, 0)$. The parameters Q and K are the strengths of the source and vortex, respectively. The parameter Q is always negative (in fact, positive values of Q define a blinking vortex-sink system). Positive and negative values of K correspond, respectively, to counterclockwise and clockwise vortex motion. The period of the flow is T, whereas Θ stands for the Heaviside step function. The sources are located at positions $(\pm 1, 0)$. For each half-period, the flow remains steady with only one of the sources open. In the time interval $0 < t \bmod T < 0.5T$, the open source is the one at $(-1, 0)$, whereas in the time interval $0.5T < t \bmod T < T$, the open source is the one at $(1, 0)$. The velocity field of the fluid flow is

$$\mathbf{u} = (u_x, u_y), \quad u_x = \partial\Psi/\partial y, \quad u_y = -\partial\Psi/\partial x. \qquad (3)$$

The blinking vortex-source system is particularly convenient for the illustration of our findings because it does not include any physical obstacle (in contrast, for instance, with the von Karman vortex street [7]). Accordingly, no interaction of the aerosols with obstacles is present. Such interactions could mask the purely dynamical effect in which we are interested. We can, therefore, isolate the chaotic saddle effects from boundary layer effects. Our trapping mechanism has, indeed, nothing to do with boundary layer effects [15].

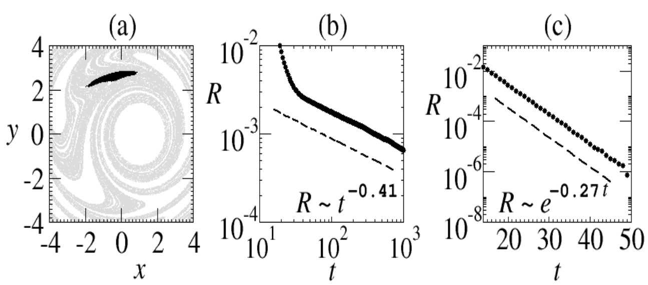

FIG. 1: Dynamics of the fluid particles. (a) KAM island (in black) and unstable manifold of the chaotic saddle (in gray) for parameters $Q = -20$, $K = -400$, and $T = 0.1$. (b) Fraction R of particles remaining in the square $[-4, 4] \times [-4, 4]$ as a function of time (black dots), for parameters $Q = -20$, $K = -400$, and $T = 0.1$. Initially, 10^6 particles were placed uniformly outside the KAM island in that domain. The algebraic decay for large t ($t > 40$) is a signature of nonhyperbolicity. (c) Fraction of particles remaining in the square $[-3, 3] \times [-3, 3]$ as a function of time (black dots), for parameters $Q = -10$, $K = -160$, and $T = 0.1$. Initially, 4×10^6 particles were placed uniformly in that domain. The exponential decay is a signature of hyperbolicity.

The parameters Q, K, and T in Eq. (2) can be chosen in order to yield either a nonhyperbolic or a hyperbolic dynamics for the fluid particles (*passive advection*). For instance, for $Q = -20$, $K = -400$, and $T = 0.1$, the invariant set is nonhyperbolic and consists of a chaotic saddle plus (at least) one KAM island. Figure 1(a) shows the major KAM island and the unstable manifold of the chaotic saddle. The algebraic decay in the number of particles in the region of the chaotic saddle, due to the *stickiness* of the island, is shown in Fig. 1(b). For $Q = -10$, $K = -160$, and $T = 0.1$, on the other hand, apparently

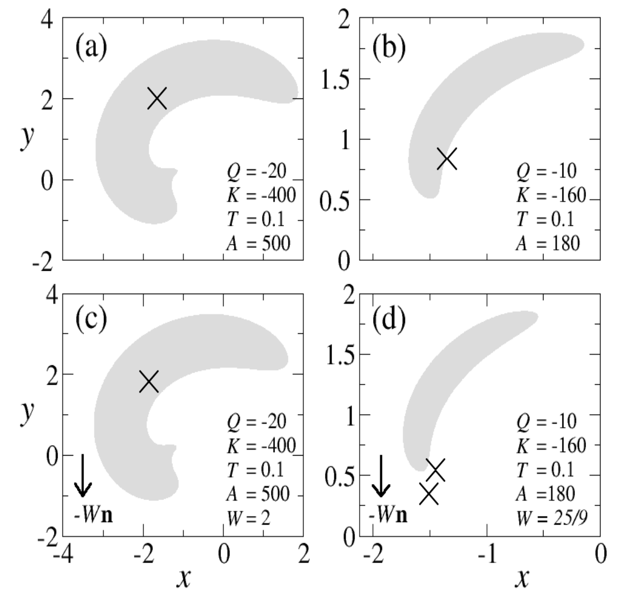

FIG. 2: Projection into the physical space of the stroboscopic section $t \bmod T = 0$ for the aerosol dynamics. The black $\times$ symbols indicate the attractors and the gray areas the corresponding basins of attraction for initial velocities equal to the local velocities of the fluid at $t = 0$. (a) Nonhyperbolic and (b) hyperbolic passive advection in the absence of gravity; (c) nonhyperbolic and (d) hyperbolic passive advection in the presence of gravity. The attractors in (a-c) are period-one orbits, whereas the attractor in (d) is a period-two orbit. Note that the attractors are not necessarily inside the gray areas because these areas correspond to *subsets* of the basins of attraction defined by specific initial velocities. The gravity vector points in the negative direction of the y-axis.

there are no islands. Indeed, Fig. 1(c) shows the exponential decay in the number of particles in the region of the chaotic saddle, a signature of hyperbolic dynamics.

We now investigate the dynamics of aerosols governed by Eq. (1) in the flow given by Eqs. (2) and (3), both in the cases where the passive advection is hyperbolic and nonhyperbolic, and both in the absence and presence of gravity. As shown in Fig. 2, the trapping of aerosols in attractors can occur in all these cases. The figure shows, for different parameters, the projection into the physical space of the attractor at time instants $t \bmod T = 0$. The corresponding basins of attraction for initial velocities equal to the local velocities of the fluid are also shown. We stress that the dynamics of the aerosols takes place in a 4-dimensional phase space, corresponding to the variables (x, y, v_x, v_y), whereas the dynamics of the fluid particles is 2-dimensional since their velocity is a function of their position. From the fluid mechanics argument that heavy particles move outwards in vortices, it is intuitive that aerosols would never be trapped when advected in open flows. Nevertheless, from the dynamical systems viewpoint, the addition of dissipation to a nonhyperbolic system may transform the KAM islands into the basins of attraction of newly formed attractors (see discussion below). Figure 2(a) shows that attractors indeed occur when the underlying passive advection is nonhyperbolic. In this case, as we are not in the weak dissipation limit, the basin of attraction is actually larger than the KAM island. Less expected is the appearance of attractors when dissipation is added to *hyperbolic* systems, which are known to be structurally stable. Notwithstanding, this outcome is also possible, as shown in Fig. 2(b), and the reason again is that we are far from the weak dissipation limit. Most surprising is the occurrence of attractors when the gravitational effects are important, i.e., when W is of order of 1 or larger. Figures 2(c) and 2(d) show that also in this case attractors can occur, and for both nonhyperbolic and hyperbolic passive advection. It is worth noting the rich variety of possibilities for the motion of aerosols under gravity, which includes both the trapping described here and the increased average settling velocity when the aerosols are in an infinite, periodic, cellular fluid flow [16].

The stroboscopic sections shown in Fig. 2 correspond to attractors that are simple periodic orbits. The full physical space projection of one such attractor is shown in Fig. 3(a). But strange attractors can also occur, as shown in Fig. 3(b). They are formed when either A or W is increased (see Fig. 4). The bifurcation diagram is dominated, in both cases, by the *period doubling route*.

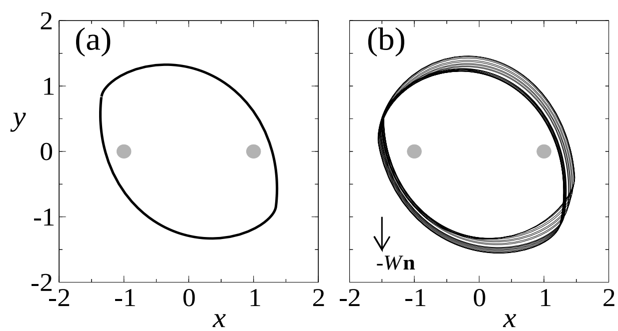

FIG. 3: (a) Periodic attractor corresponding to $W = 0$ and (b) strange attractor corresponding to $W = 40/9$. The gray dots represent the point sources. The unspecified parameters are the same as in Fig. 2(b).

The trapping of aerosols in open flows displaying chaotic advection is a general phenomenon. The dynamics defined by Eq. (1) is dissipative. In open flows, dissipation is not a sufficient condition for the occurrence of attractors. However, this condition becomes sufficient if a set of initial conditions with positive volume is advected back to itself after a certain time. In the case of bubbles, this condition is frequently satisfied because bubbles tend to remain inside closed orbits of the fluid particles generated by vortices [11]. This mechanism cannot explain the existence of attractors in the case of aerosols because, for heavy particles, rather the opposite happens due to

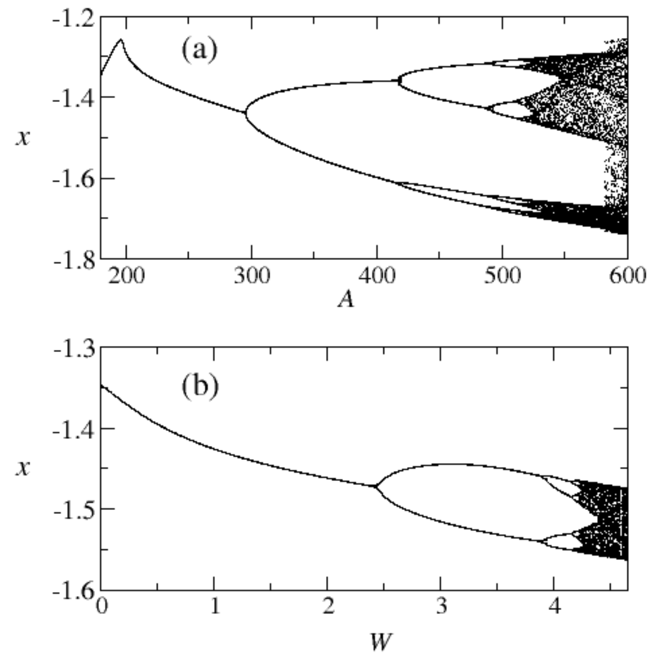

FIG. 4: Bifurcation diagrams showing the x-coordinates of the attractor at time t mod $T = 0$ (a) as a function of the parameter A in the absence of gravity and (b) as a function of W when $A = 180$. The unspecified parameters are the same as in Fig. 2(b).

the centrifugal force. However, when *multiple* vortices are present in the flow, we show that a different mechanism can give rise to attractors in which the aerosols are trapped.

The mechanism of trapping is in this case based on successive "escape attempts" from distinct vortices. As shown in Fig. 5, a possible outcome of the motion of aerosols outwards successive vortices is the formation of bounded orbits. In the case of the blinking vortex system, we have shown numerically that this occurs for a set of orbits with positive volume. For nonhyperbolic passive advection, we can demonstrate the formation of attractors explicitly for $A \gg 1$ and $W \ll 1$ using a first-order approximation [17] of the dynamics given by $\dot{\mathbf{r}} = \mathbf{u} - W\mathbf{n} - \frac{1}{A}[\frac{\partial \mathbf{u}}{\partial t} + (\mathbf{u}\cdot\nabla)\mathbf{u} - (W\mathbf{n}\cdot\nabla)\mathbf{u}]$. If $W \ll 1$ and the magnitude of the term inside the brackets is much smaller than A, the dynamics corresponds to a small perturbation of the passive advection in a 2-dimensional effective phase space. If the divergence $\nabla\cdot\dot{\mathbf{r}}$ of the velocity field is negative, as in the blinking vortex-source system [18], KAM islands of the passive advection are expected to be transformed into basins of attractions. The formation of attractors in KAM islands has been observed in the advection of bubbles and in the study of Hamiltonian systems [19]. However, in contrast with the mechanism previously considered in the study of bubbles, in the case of aerosols the KAM islands that give rise to attractors describe the dynamics of particles that are excluded from remaining confined to a single vortex. From the relation $\nabla\cdot\dot{\mathbf{r}} = (\omega^2 - s^2)/(2A)$ [17], we can see that in these islands the strain s must dominate over the vorticity ω. Furthermore, we emphasize that the phenomenon of trapping of aerosols is far more general since it also occurs in non-perturbative regimes (small A and large W) and in the absence of KAM islands, as shown in Figs. 2-5.

In conclusion, we have demonstrated the counterintuitive occurrence of trapping of heavy particles in open flows. This phenomenon does not depend on the nonhyperbolicity of the passive advection and is possible even when the gravitational effect is large. The trapping of aerosols that we found here for spatially smooth *open* flows has analogies with the suspension of heavy particles in turbulent *closed* flows reported in Ref. [20]. But one difference is that in the results presented in this Letter the trapping is permanent, whereas the random time dependence makes the trapping transient in the case of turbulence. Our findings are particularly surprising because they refer to open flows and show that aerosols can be trapped under gravity even when *almost all* the particles of fluid escape from the domain of interest. This phenomenon is expected to be useful for particle separation purposes in microflows [21].

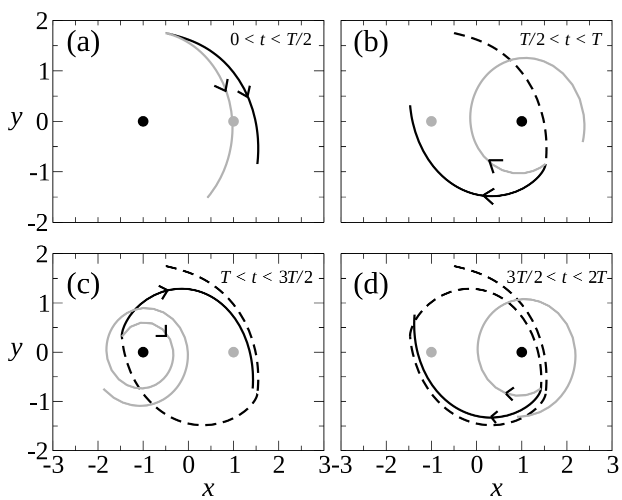

FIG. 5: Trajectories of an aerosol (black) and a fluid particle (gray) of same initial position, and also of same initial velocity in (a). The point source that is open during each time interval is shown as a black dot (the gray dot corresponds to the other one). The dashed lines represent the trajectory of the aerosol before the time interval indicated in the figure. The parameters are the same as in Fig. 2(b). After 2 periods of the fluid flow, the aerosol is already very close to a periodic attractor [cf. Fig. 3(a)].

The authors thank Tamás Tél for stimulating discussions.

* Electronic address: rdvilela@pks.mpg.de

[1] M.A. Stremler, F.R. Haselton, and H. Aref, Phil. Trans. R. Soc. Lond. A **362**, 1019 (2004).
[2] P. Haynes, *Mixing: Chaos and Turbulence*, edited by H. Chaté *et al.* (Kluwer Academic/Plenum Publishers, New York, 1999), p. 229-272.
[3] P. Yager *et al.*, Nature (London) **442**, 412 (2006); M. Toner and D. Irimia, Annual Review of Biomedical Engineering **7**, 77 (2005).
[4] J.H. Seinfeld, *Atmospheric Chemistry and Physics* (Wiley, New York, 1998).
[5] T. Tél, T. Nishikawa, A.E. Motter, C. Grebogi, and Z. Toroczkai, Chaos **14**, 72 (2004); T. Tél, A. de Moura, C. Grebogi, and G. Károlyi, Phys. Rep. **413**, 91 (2005).
[6] E.R. Abraham, Nature (London) **391**, 577 (1998); I. Scheuring, G. Károlyi, A. Pentek, T. Tél, and Z. Toroczkai, Freshwater Biology **45**, 123 (2000); C. López, Z. Neufeld, E. Hernández-García, and P.H. Haynes, Phys. Chem. Earth (B) **26**, 313 (2001); R. Reigada *et al.*, Proc. R. Soc. Lond. B **270**, 875 (2003).
[7] C. Jung, T. Tél, and E. Ziemniak, Chaos **3**, 555 (1993).
[8] H. Kantz and P. Grassberger, Physica (Amsterdam) **17D**, 75 (1985); T. Tél, in *Directions in Chaos*, edited by Hao Bai-Lin, (World Scientific, Singapore, 1990), Vol. 3, pp. 149-221.
[9] J.M. Ottino, *The Kinematics of Mixing: Stretching, Chaos, and Transport* (Cambridge University Press, Cambridge, 1989).
[10] J.C. Sommerer and E. Ott, Science **259**, 335 (1993); L. Yu, E. Ott, and Q. Chen, Physica D **110**, 1 (1997).
[11] I.J. Benczik, Z. Toroczkai, and T. Tél, Phys. Rev. Lett. **89**, 164501 (2002); Phys. Rev. E. **67**, 036303 (2003).
[12] A.E. Motter, Y.-C. Lai, and C. Grebogi, Phys. Rev. E **68**, 056307 (2003).
[13] M.R. Maxey and J.J. Riley, Phys. Fluids. **26**, 883 (1983); T.R. Auton, J.C.R. Hunt, and M. Prud'homme, J. Fluid. Mech. **197**, 241 (1988); E.E. Michaelides, J. Fluids Eng. **119**, 233 (1997).
[14] H. Aref, S.W. Jones, S. Mofina, and I. Zawadzki, Physica (Amsterdam) **37D**, 423 (1989); G. Károlyi and T. Tél, Phys. Rep. **290**, 125 (1997).
[15] C. Marchioli and A. Soldati, J. Fluid. Mech. **468**, 283 (2002).
[16] M.R. Maxey and S. Corrsin, J. Atmos. Sci. **43**, 1112 (1986).
[17] M.R. Maxey, J. Fluid Mech. **174**, 441 (1987).
[18] For the blinking vortex-source system, we find $\nabla\cdot\dot{\mathbf{r}} = -\frac{2(K^2+Q^2)}{A}\left[\frac{1}{r'^4}\Theta(\tau)+\frac{1}{r''^4}\Theta(-\tau)\right] < 0$.
[19] M.A. Lieberman and K.Y. Tsang, Phys. Rev. Lett **55**, 908 (1985); T. Pohl, U. Feudel, and W. Ebeling, Phys. Rev. E **65**, 046228 (2002); A.E. Motter and Y.-C. Lai, Phys. Rev. E **65**, 015205 (2002).
[20] C. Pasquero, A. Provenzale, and E.A. Spiegel, Phys. Rev. Lett. **91**, 054502 (2003).
[21] J. Yang *et al.*, Anal. Chem. **71**, 911 (1999); M. Kostur *et al.*, Phys. Rev. Lett. **96**, 014502 (2006).

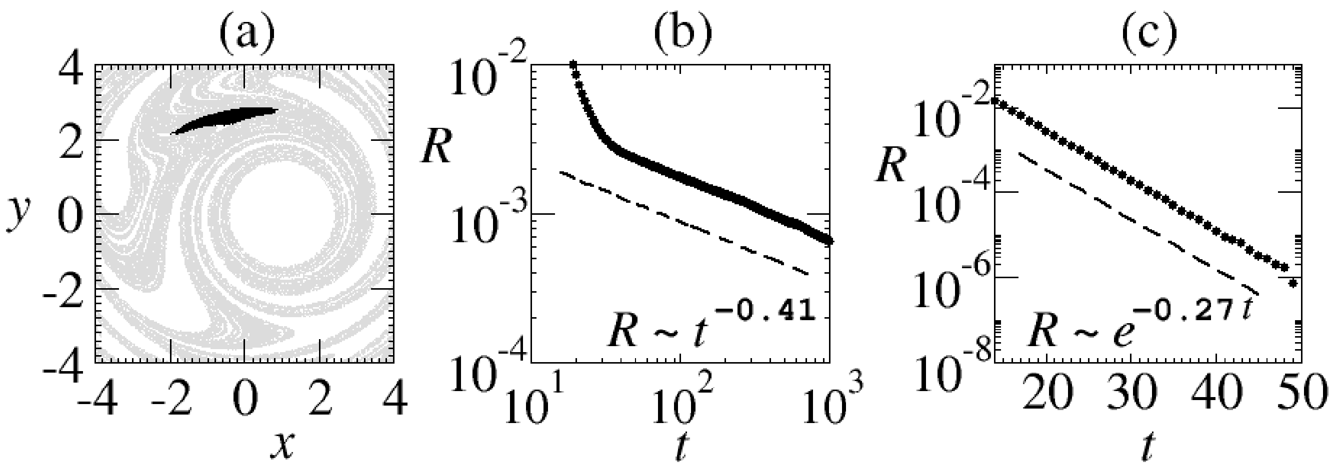

Figure 1

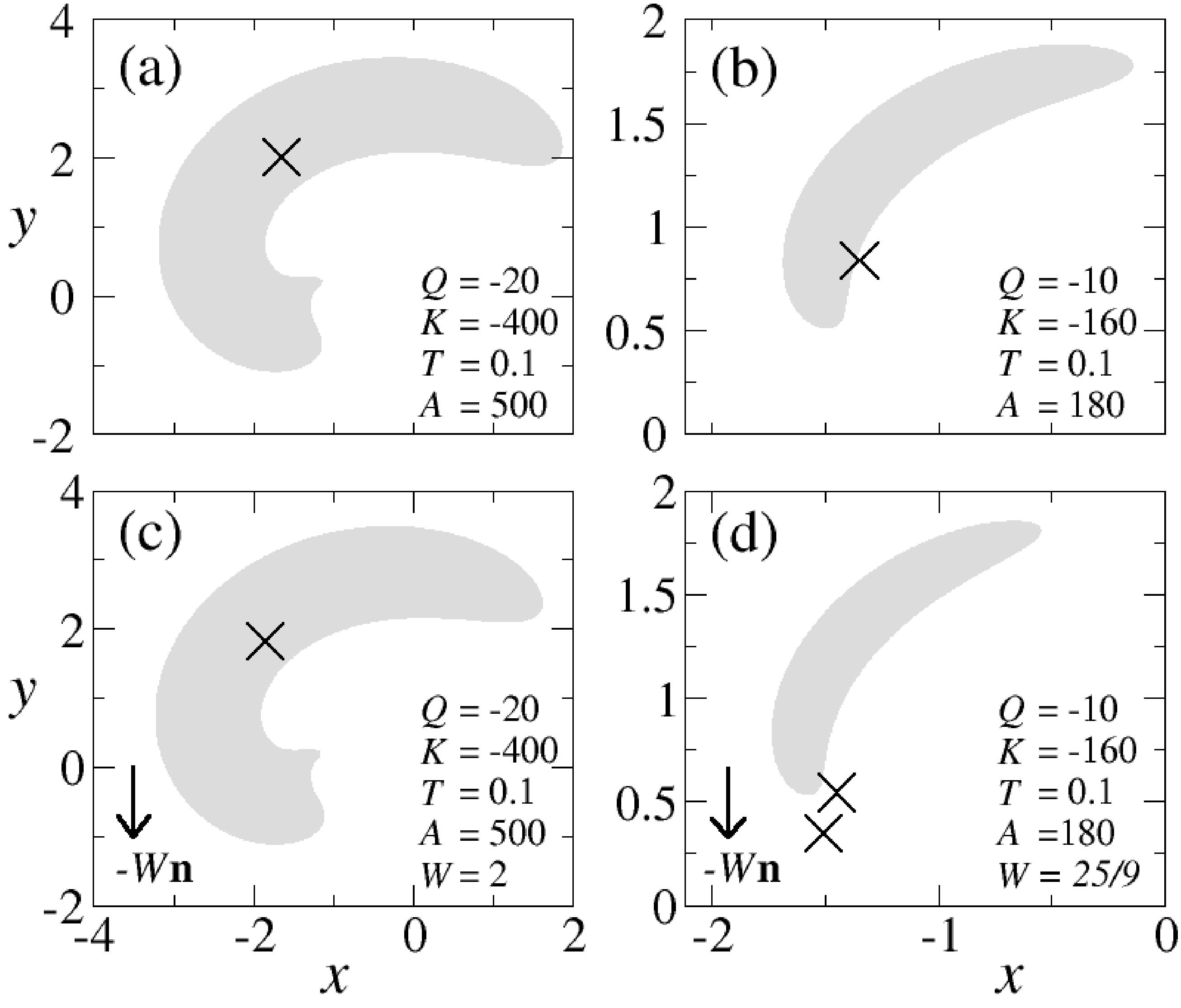

(a)
Q = -20
K = -400
T = 0.1
A = 500
(b)
Q = -10
K = -160
T = 0.1
A = 180
(c)
Q = -20
K = -400
T = 0.1
A = 500
W = 2
-Wn
(d)
Q = -10
K = -160
T = 0.1
A =180
W = 25/9
-Wn
x
y

Figure 2

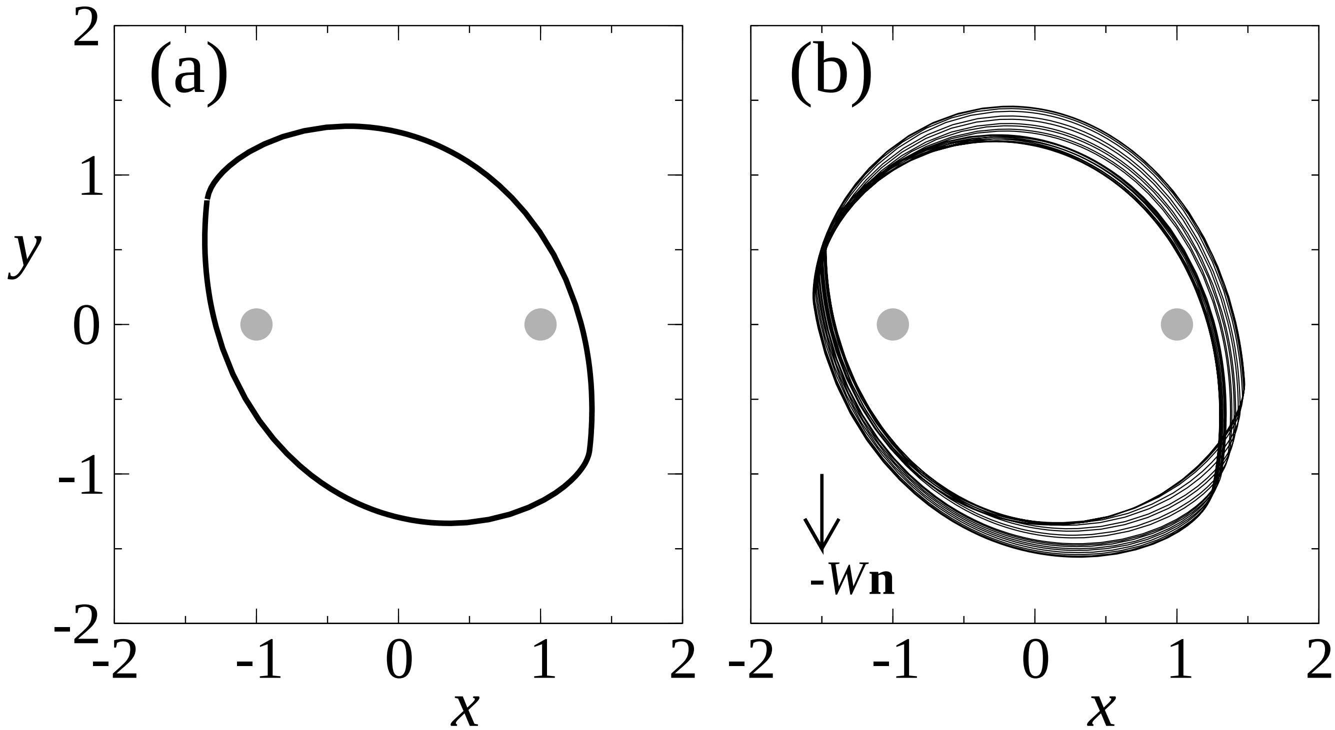

Figure 3

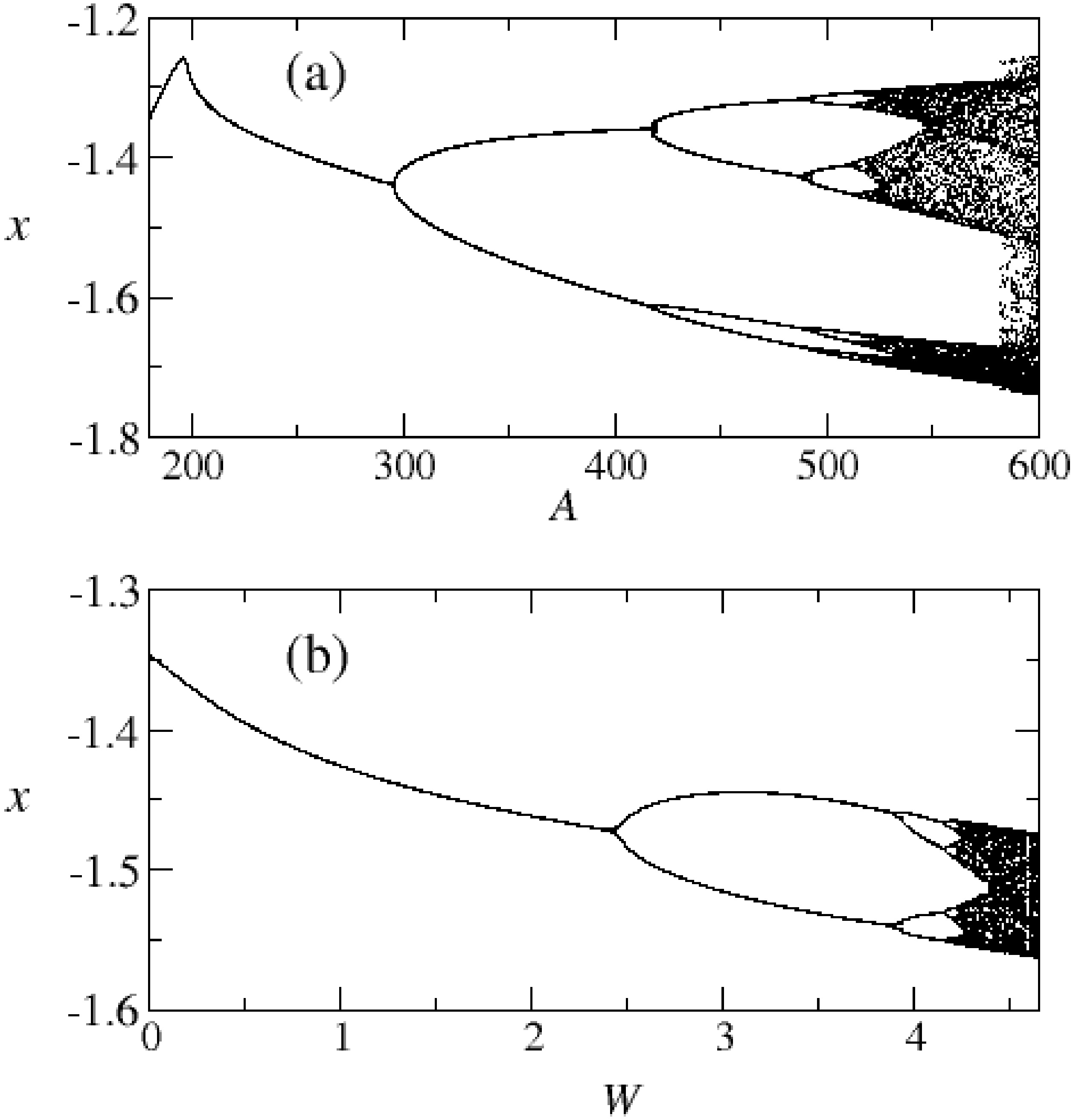

Figure 4

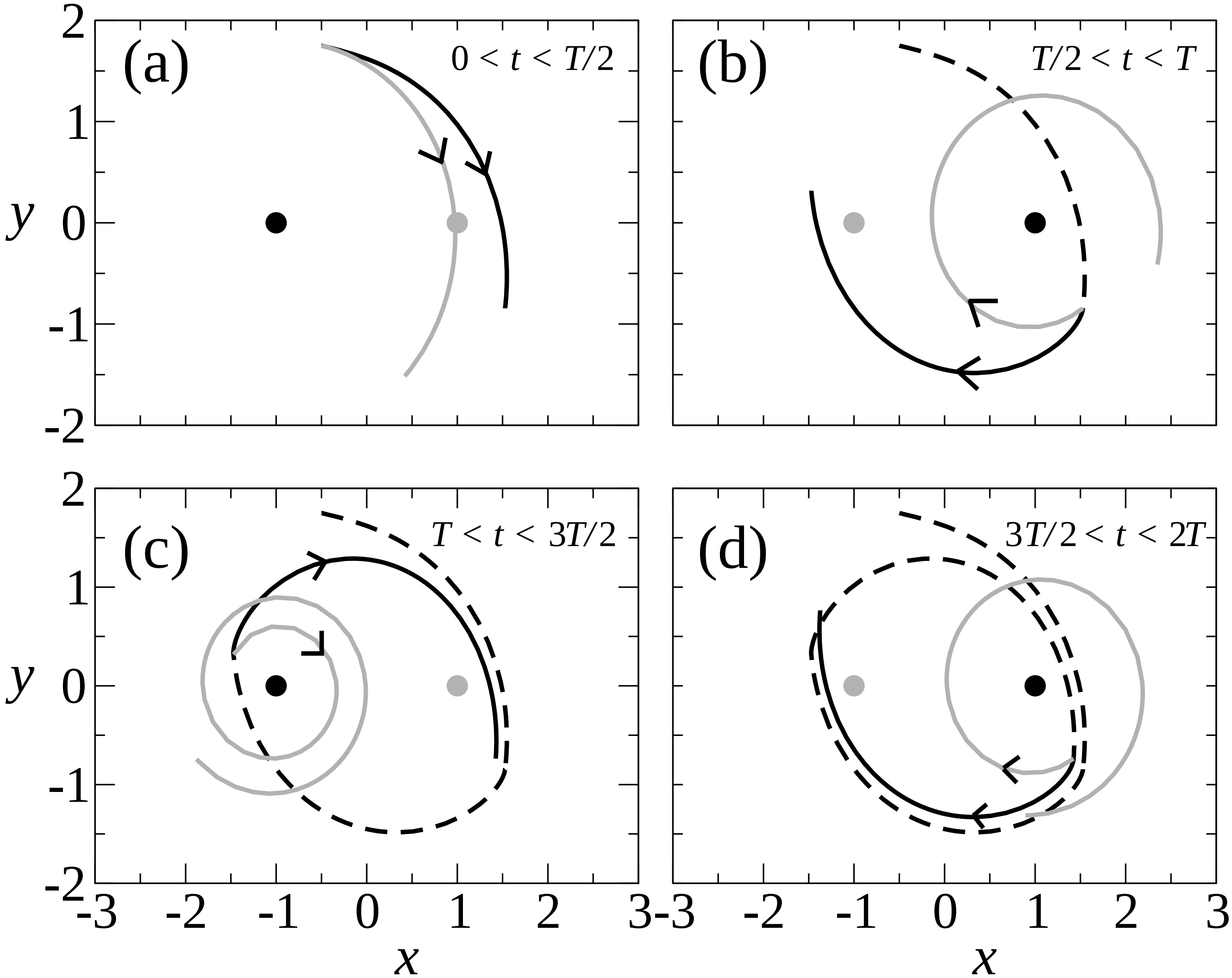

Figure 5